Development of Effective Antivirals

4

Identification of Novel Inhibitor of SARS-CoV-2 Plpro

Rimanshee Arya[1,2], Janani Ganesh[1,2], Vishal Prashar*[1,2] and Mukesh Kumar*[1,2]

[1]*Protein Crystallography Section, Bio-Science Group, Bhabha Atomic Research Centre (BARC), Trombay-400085, INDIA*
[2]*Homi Bhabha National Institute, Anushakti Nagar, Mumbai-400094, INDIA*

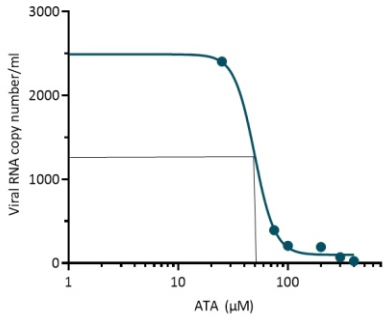

In vitro IC_{50} determination of ATA

ABSTRACT

The papain-like protease (PLpro) of SARS-CoV-2 is an important drug target against COVID-19 due to its essential role in viral replication and modulation of host immune responses. With the virus undergoing mutations across its genome, there's a pressing need for effective antivirals to combat the disease and its potential future outbreaks. In this study, we conducted screening of small molecule libraries to identify potential PLpro inhibitors. We found that aurintricarboxylic acid (ATA) inhibits PLpro, with K_i and IC_{50} values of 16 μM and 30 μM, respectively. The thermodynamics of ATA binding to PLpro were further characterized using isothermal titration calorimetry. *In vitro* assays demonstrated the antiviral efficacy of ATA with IC_{50} of 50 μM. Subsequently, its *in vivo* antiviral potential was also studied in Syrian hamsters.

KEYWORDS: *SARS-CoV-2, COVID, Aurintricarboxylic acid, PLpro, Papain-like protease, Antiviral*

Introduction

Developing effective antivirals against SARS-CoV-2 is crucial for managing the COVID-19 disease and preparing for potential future coronavirus outbreaks. Targeting essential steps in the virus's life cycle, such as blocking the interaction between the viral spike protein and the host ACE2 receptor, inhibiting viral genome replication by targeting viral RNA-dependent RNA polymerase (RdRp), and inhibiting viral proteases like the main protease and the papain-like protease (PLpro), are key strategies for drug development [1-3].

Papain like protease (PLpro) of SARS-CoV-2 cleaves viral polyproteins (pp1a/1ab) at three sites to yield mature non-structural proteins, Nsp1, Nsp2, and Nsp3, essential for virus replication. Besides, PLpro is also implicated in the evasion of host antiviral immune responses through deubiquitination and deISG15lation of several host/viral proteins hampering the signalling cascades of the innate immune system [4-7]. Therefore, inhibition of PLpro will not only suppress the viral multiplication but also help in overcoming the dysregulation of host innate immune response caused by viral infection. While several potential PLpro inhibitors have been identified previously, their clinical efficacy remains limited. Therefore, there is a need to find novel PLpro inhibitors.

In this study, employing our previously established optimized assay conditions [8], we undertook a high-throughput biochemical screening with small molecule libraries to identify novel inhibitors of SARS-CoV-2 PLpro. Among the compounds screened, aurintricarboxylic acid (ATA) emerged as a potent inhibitor of the PLpro enzyme with inhibition constant in the low micromolar range.

Subsequently, we explored the potential of ATA in inhibiting PLpro both *in vitro* and *in vivo*.

**Authors for Correspondence: Vishal Prashar and Mukesh Kumar*
E-mail: vishalp@barc.gov.in and mukeshk@barc.gov.in

Materials and Methods

Expression and purification of PLpro: The recombinant protein of SARS-CoV-2 PLpro was expressed and purified as previously described [8]. Briefly, the protein was expressed in BL21(DE3) strain of *E. coli* and purified from the soluble fraction of the cell lysate using Nickel-affinity chromatography followed by size exclusion chromatography. The purified protein, concentrated to 10 mg/ml, was stored at 4°C in a storage buffer (50 mM HEPES pH 7.5, 100 mM NaCl, and 5 mM DTT) for further studies.

High throughput screening: The experiments were conducted using 96-well black non-treated plates (Thermo Scientific, Denmark) in a CLARIOstar Plus multi-mode microplate reader (BMG Labtech, Germany), with excitation and emission filters set at 355 nm and 430 nm, respectively. The assay buffer consisted of 50 mM MES (pH 6.5), 100 mM NaCl, 0.5 mM EDTA, 5 mM DTT, and 0.1 mg/ml BSA. Initial screening assays were performed in a reaction volume of 50 μl, comprising 200 nM enzyme, 300 μM test compound, and 20 μM fluorogenic tetrapeptide substrate (Z-Leu-Arg-Gly-Gly-AMC). IC_{50} values were determined through three/four parameters non-linear regression fitting of velocity data for different compound concentrations (0-300 μM) at a fixed concentration of the substrate (20 μM) using GraphPad Prism software (www.graphpad.com). The plotted data in Fig.1 (a,b) represent mean values derived from three independent experiments.

Isothermal Titration calorimetry: Isothermal titration calorimetry (ITC) experiments were performed to study thermodynamics of PLpro-ATA interaction using MicroCal iTC200 instrument (Malvern Panalytical Ltd., UK). Protein and ATA were used at concentrations of 25 μM and 0.7 mM, respectively in Tris (pH 7.5), 100 mM NaCl, and 5 mM DTT. Sample cell contained the protein with temperature and reference power set at 25°C and 5 μcal/sec, respectively. Each titration with ATA comprised an initial injection of 0.4 μl

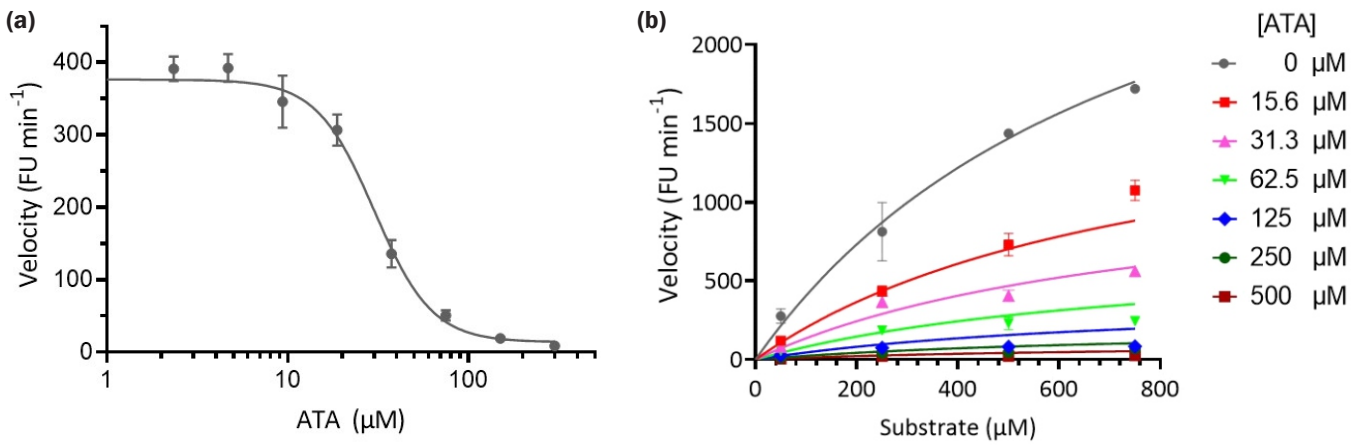

Fig.1: Biochemical characterization of PLpro inhibition by ATA (a) Concentration-dependent inhibition of PLpro enzymatic activity by ATA; [PLpro]=200nM, [Substrate]=70µM; (b) Enzymatic activity of PLpro at different concentrations of Z-LRGG-AMC substrate (50, 250, 500, 750 µM) and ATA (0-500 µM) to estimate K_i. FU: Fluorescence units.

followed by 18 identical injections of 2 µl, lasting 4 seconds per injection, and spaced 120 seconds apart. An initial delay of 120 seconds was applied, with stirring at 800 rpm. The heat of dilution derived from ATA titration in buffer was averaged and subtracted from each injection. Interaction parameters were computed using MicroCal iTC200 analysis software.

In vitro toxicity and antiviral assay of ATA: Before proceeding for in vitro antiviral assay, cytotoxicity assessment of ATA against Vero E6 cells was carried out. After seeding cells in a 96-well plate at 80% confluency, various concentrations of ATA (up to 1 mM) were added. MTT assay was performed after 48 hours to gauge cell viability. For the antiviral assay, Vero E6 cells, similarly seeded in a 96-well plate at 80% confluency, were infected with SARS-CoV-2 at 0.1 m.o.i. for two hours. Post-infection, different concentrations of ATA (ranging from 25 to 400 µM) in fresh media were added to the cells. Supernatants were collected at 24 hours post-infection, and RNA isolation followed by RT-qPCR analysis using specific primers for viral spike, nucleocapsid, and ORF1a was conducted. Mean Ct values from the RT-qPCR were utilized to estimate viral RNA copy numbers, and IC_{50} for ATA was determined using GraphPad Prism with four parameters variable slope non-linear regression fitting.

Evaluation of antiviral potential of ATA in Syrian hamsters: The antiviral efficacy of ATA was evaluated *in vivo* in 24 Syrian hamsters, divided into four groups of six animals each: one control and three treatment. All animals were intra-nasally infected with SARS-CoV-2 ($TCID_{50}$ = 10^5) on day zero. While the control group received no treatment, the treatment groups (A, B, and C) were administered ATA at doses of 15, 30, and 45 mg/kg body weight, respectively, starting four hours post-infection via oral route in a 100 µl solution. Dosages were repeated daily for four days (day 1-4), and animals were euthanized on day 5. Daily monitoring and recording of body weights were conducted throughout the study. Throat swabs and lung tissues were collected from all the animals for further analysis. RT-qPCR was employed to estimate the viral loads in throat swabs and left lung tissues, while histopathological evaluations were performed on the right lung tissues. Statistical analysis to determine differences among groups was conducted using Welch's t-test (one-tailed).

Results

High throughput screening

A screening of 350 drug-like compounds, including natural product compounds, was carried out against PLpro under optimized assay conditions as previously reported [8]. Significant inhibition of the enzyme was observed only with ATA. Concentration-dependent inhibition of PLpro enzymatic activity revealed an IC_{50} value of 30 µM for ATA (Fig.1(a)). To ascertain the type of inhibition and the inhibitory constant (*Ki*), enzymatic assays were performed at four substrate concentrations (50, 250, 500, 750 µM) with varying ATA concentrations (0 µM – 500 µM) (Fig.1(b)). The kinetic data were analysed using SigmaPlot software, fitting them into four models of enzyme inhibition (competitive, non-competitive, uncompetitive, and mixed). The Akaike Information Criterion corrected (AICc) values were employed to determine the most plausible mode of inhibition. The kinetic data demonstrated the best fit with the non-competitive model of enzyme inhibition, yielding a *Ki* value of 16 µM.

Isothermal titration calorimetry

The binding energetics of ATA to PLpro were investigated using isothermal titration calorimetry (ITC) (Fig.2). Analysis of thermodynamic data, fitted into a one-site binding model, revealed a dissociation constant (K_D) of 11.3 µM with enthalpy (ΔH) and entropy (ΔS) changes of -2.47 kcal/mol and 14.3 cal/mol/deg, respectively. These thermodynamic findings indicate favourable contributions from both enthalpy and entropy to the overall binding energy (ΔG), suggesting that the interaction between ATA and PLpro involves a combination of hydrophobic and hydrogen bonding interactions.

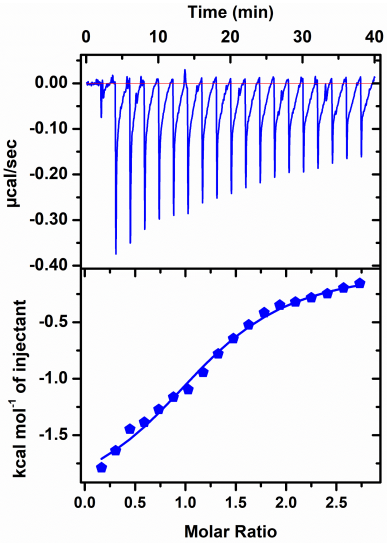

Fig.2: Thermodynamic and kinetic parameters of ATA binding to PLpro. Top panel: Raw data of calorimetric titration showing exothermic heat changes with successive injections; Bottom panel: Integrated binding isotherm plotted against molar ratio (ATA: Plpro).

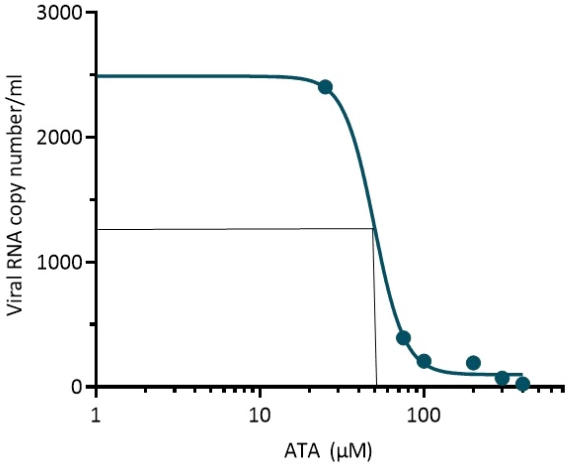

Fig.3: In vitro IC_{50} determination of ATA.

In vitro toxicity and antiviral potential of ATA

The *in vitro* antiviral potential of ATA was explored by first assessing its cytotoxicity in Vero E6 cells. Treatment with 1.0 mM ATA showed 95% cell viability after 48 hours, indicating its non-toxic nature at this concentration. Subsequently, antiviral efficacy of ATA was evaluated at concentrations below 1.0 mM. Vero E6 cells infected with SARS-CoV-2 were treated with different ATA concentrations (ranging from 0 to 400 μM). The viral load, estimated in terms of viral RNA copy numbers via RT-qPCR, exhibited a notable reduction as ATA concentration increased from 25 μM to 75 μM, indicating an IC_{50} value between these concentrations. Using four-parameter variable slope non-linear regression fitting, the IC_{50} was determined as 50 μM (Fig.3).

Evaluation of in vivo antiviral potential of ATA in Syrian hamsters

The *in vivo* antiviral efficacy of ATA was assessed in Syrian hamsters using a previously established protocol [9]. ATA was orally administered to SARS-CoV-2-infected animals in three treatment groups, designated as (a), (b), and (c), at doses of 15, 30, and 45 mg/kg body weight, respectively. The treatment schedule for ATA is illustrated in Fig.4(a).

Throughout the five-day observation period, no notable weight loss, complications, or mortality occurred in any groups (treatment or untreated controls). RT-qPCR analysis revealed a decrease in virus RNA copy numbers in throat swab samples from ATA-treated groups compared to the untreated control (Fig.4(b)). Significance of this reduction was determined using one-tailed Welch's t-test, showing a 0.4-log reduction in groups A and B (*p*-values: 0.0592 and 0.0580, respectively) and a 1-log reduction in group C (*p*-value: 0.0439) compared to the untreated control.

However, in lung tissues, no significant reduction in virus RNA levels was observed in the treatment groups compared to the untreated control (Fig.4(c)). Additionally, there were no noticeable differences in lung pathology between the untreated and ATA-treated groups.

Conclusion

In this study, we have screened a library of compounds using high-throughput biochemical assay to find potential inhibitors of SARS-CoV-2 PLpro. ATA emerged as a promising inhibitor of PLpro. Further, its binding parameters were assessed through biochemical and biophysical methods. We also evaluated its in vitro antiviral efficacy against SARS-CoV-2 using viral culture in VeroE6 cells. Subsequent *in vivo*

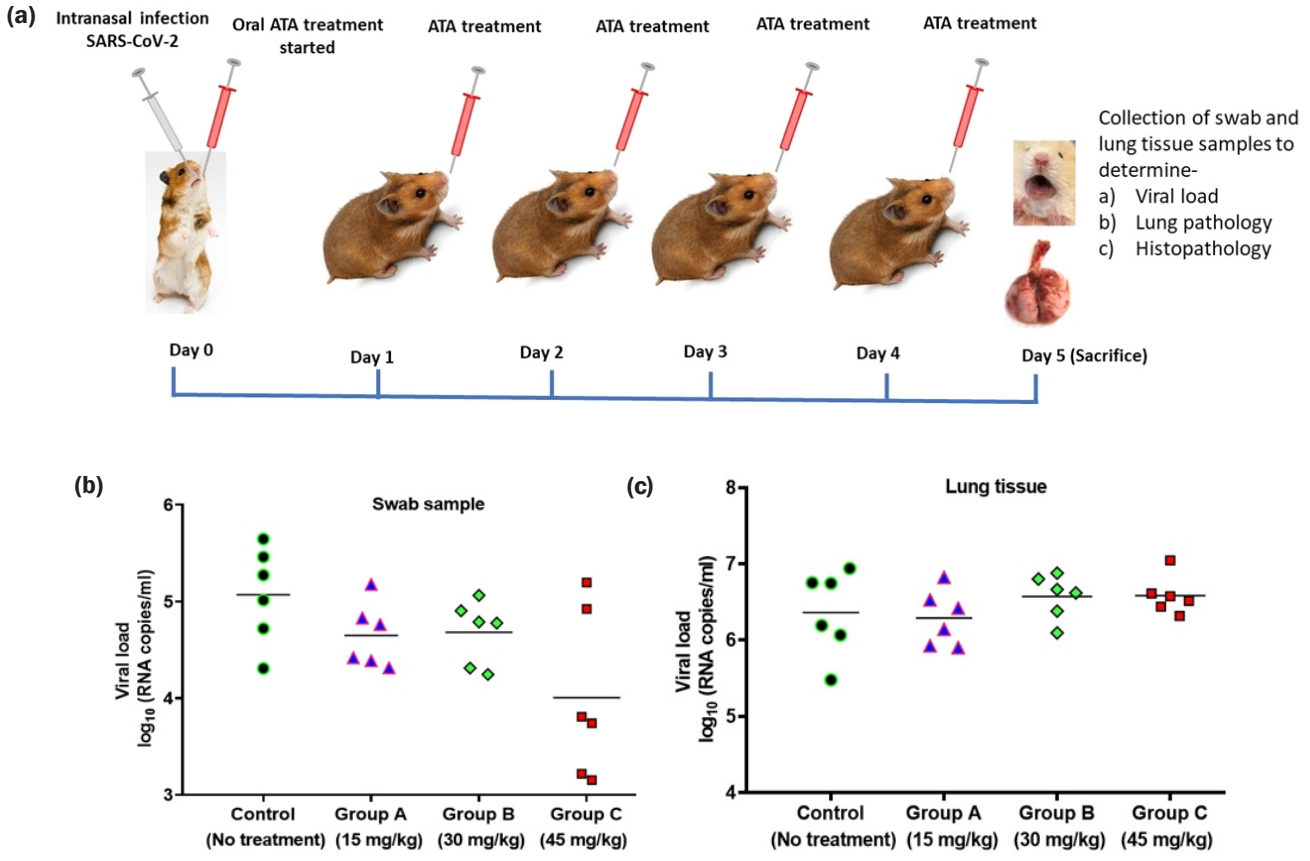

Fig.4: In vivo antiviral assay of ATA. (a) Treatment design in Syrian hamsters. (b) Throat swabs and (c) Lung tissues of SARS-CoV-2-infected animals from the untreated control (six animals) and three treatment groups (six animals each). Horizontal bars represent mean values.

investigations in SARS-CoV-2-infected Syrian hamsters demonstrated that oral administration of ATA led to a reduction in viral load in the throat. However, no discernible improvement in lung pathology was observed, possibly due to limited cell permeability of ATA. However, ATA's low toxicity suggests its potential as an oral gargle or nasal cleaning solution to reduce viral transmission. Alternative administration routes, like nebulization or nasal inhalation, may enhance bioavailability of ATA in lung tissues.

Acknowledgments

We express our gratitude to the Biovalidation services and the ABSL-3 facility of the Institute of Life Sciences, Bhubaneshwar, India for providing professional services for *in vitro* and *in vivo* evaluation of antiviral activity of ATA. We also extend our sincere thanks to Dr. S.K. Nayak, Dr. S.K. Ghosh, Dr. Kshama Kundu, Dr. Soumyaditya Mula, Dr. Prasad P. Phadnis, Dr. Chander P. Kaushik, Dr. Sudip Gorai, and Dr. Kartik Dutta for kindly providing their synthesized compounds for high-throughput screening against PLpro.

References

[1] B. Hu, H. Guo, P. Zhou, Z.-L. Shi, Characteristics of SARS-CoV-2 and COVID-19, Nature Reviews Microbiology. 19 (2021) 141–154. https://doi.org/10.1038/s41579-020-00459-7.

[2] P. V'kovski, A. Kratzel, S. Steiner, H. Stalder, V. Thiel, Coronavirus biology and replication: implications for SARS-CoV-2, Nat Rev Microbiol. 19 (2021) 155–170. https://doi.org/10.1038/s41579-020-00468-6.

[3] R. Arya, S. Kumari, B. Pandey, H. Mistry, S.C. Bihani, A. Das, V. Prashar, G.D. Gupta, L. Panicker, M. Kumar, Structural insights into SARS-CoV-2 proteins, J Mol Biol. 433 (2021) 166725. https://doi.org/10.1016/j.jmb.2020.11.024.

[4] M. Zhang, J. Li, H. Yan, J. Huang, F. Wang, T. Liu, L. Zeng, F. Zhou, ISGylation in Innate Antiviral Immunity and Pathogen Defense Responses: A Review, Front. Cell Dev. Biol. 9 (2021) 788410. https://doi.org/10.3389/fcell.2021.788410.

[5] D. Shin, R. Mukherjee, D. Grewe, D. Bojkova, K. Baek, A. Bhattacharya, L. Schulz, M. Widera, A.R. Mehdipour, G. Tascher, P.P. Geurink, A. Wilhelm, G.J. van der Heden van Noort, H. Ovaa, S. Müller, K.-P. Knobeloch, K. Rajalingam, B.A. Schulman, J. Cinatl, G. Hummer, S. Ciesek, I. Dikic, Papain-like protease regulates SARS-CoV-2 viral spread and innate immunity., Nature. 587 (2020) 657–662. https://doi.org/10.1038/s41586-020-2601-5.

[6] H. Hu, S.-C. Sun, Ubiquitin signaling in immune responses, Cell Research. 26 (2016) 457–483. https://doi.org/10.1038/cr.2016.40.

[7] D. Munnur, Q. Teo, D. Eggermont, H.H.Y. Lee, F. Thery, J. Ho, S.W. van Leur, W.W.S. Ng, L.Y.L. Siu, A. Beling, H. Ploegh, A. Pinto-Fernandez, A. Damianou, B. Kessler, F. Impens, C.K.P. Mok, S. Sanyal, Altered ISGylation drives aberrant macrophage-dependent immune responses during SARS-CoV-2 infection, Nat Immunol. 22 (2021) 1416–1427. https://doi.org/10.1038/s41590-021-01035-8.

[8] R. Arya, V. Prashar, M. Kumar, Evaluating Stability and Activity of SARS-CoV-2 PLpro for High-throughput Screening of Inhibitors, Molecular Biotechnology. 64 (2022) 1–8. https://doi.org/10.1007/s12033-021-00383-y.

[9] V. Suresh, V. Mohanty, K. Avula, A. Ghosh, B. Singh, R.K. Reddy, D. Parida, A.R. Suryawanshi, S.K. Raghav, S. Chattopadhyay, P. Prasad, R.K. Swain, R. Dash, A. Parida, G.H. Syed, S. Senapati, Quantitative proteomics of hamster lung tissues infected with SARS-CoV-2 reveal host factors having implication in the disease pathogenesis and severity, The FASEB Journal. 35 (2021) e21713. https://doi.org/10.1096/fj.202100431R.